ARMY RESEARCH LABORATORY

On Propellant Surface Temperatures Derived From Calorimetry

John A. Vanderhoff and Michael McQuaid

ARL-TR-2434 March 2001

The findings in this report are not to be construed as an official Department of the Army position unless so designated by other authorized documents.

Citation of manufacturer's or trade names does not constitute an official endorsement or approval of the use thereof.

Destroy this report when it is no longer needed. Do not return it to the originator.

Army Research Laboratory
Aberdeen Proving Ground, MD 21005-5067

ARL-TR-2434 **March 2001**

On Propellant Surface Temperatures Derived From Calorimetry

John A. Vanderhoff and Michael McQuaid
Weapons and Materials Research Directorate, ARL

Abstract

Propellant surface temperatures for double base (JA2) and nitramine (XM39) propellant samples burning at pressures from 0.8 to 4 MPa have been measured using two different calorimetric techniques. The methods differ in the way combustion is extinguished; one involves depressurization, and the other involves burning into an inert base. For the experiments based on depressurization, a main source of uncertainty was in determining the area of the combusting surface. Moreover, this technique was prone to a large number of unproductive runs. Most of the data presented here was obtained from experiments in which combustion was extinguished by burning into a PolyEtherEtherKetone (PEEK) base. This robust material has thermophysical properties similar to the propellants studied. At higher pressures (and mass regression rates), radiative heating made nonnegligible contributions to total heat input to the inert base. Thus, a multivariate least squares model was developed to describe a time-dependent radiative and conductive heat input, and it was used to fit the experimental temperature histories. Propellant surface temperatures, radiative fluxes, and optical absorption coefficients are obtained from the fit to the data. For the regions of low mass regression rates (< 0.7 g/cm^2-s), the propellant surface temperatures were in agreement with published values. At larger mass regression rates, the propellant surface temperatures were larger than published values. This was believed to be a consequence of the way contributions from radiative heating were treated.

Acknowledgments

The authors thank Peter Dehmer for hot pressing the PEEK material to create the inert base and Jeffrey Morris for measuring the FTIR optical absorption spectra from which the absorption coefficient for PEEK was determined.

INTENTIONALLY LEFT BLANK.

Contents

List of Figures

List of Tables

INTENTIONALLY LEFT BLANK.

1. Introduction

A wealth of information about the combustion characteristics of a propellant can be derived from accurately determining the spatial temperature profile for a steady-state burning process [1-3]. A key boundary condition in this profile is the temperature of the combusting surface. This boundary condition, when given as a function of the mass regression rate, can be used to characterize condensed phase kinetics [1]. Over time, microthermocouples have emerged as the standard technique for determining temperature profiles [1-4]. However, because the temperature gradients are large, the accuracy of obtaining the surface temperature with this technique can be dominated by uncertainties in surface position.

Despite the current preeminence of the microthermocouple technique, one of the earliest measurements of propellant surface temperature was made by Aristova and Leipunskiy [5], who used a calorimeter to measure the heat content of an extinguished propellant sample. Based on this technique, these researchers obtained surface temperatures of 525 K and 603 K, respectively, for pyroxylin (double-base propellant) and nitroglycerin powders burning at 1 atm. Uncertainties were reported to be ± 45K. For the pyroxylin case, the experiment consisted of dropping the combusting pyroxylin through a CO_2 cloud (extinguishing the combustion in a 1-atm environment) and into a small, liquid-filled dewar calorimeter. The temperature rise of the liquid in the calorimeter was one of the central measurements of the experiment.

After reading about this work, several ideas surfaced about how to modify the experiment to measure the propellant surface temperature at elevated pressures. The motivation for proceeding with a calorimetric technique was to remove ambiguities of surface-microthermocouple distance and to relax the fast response time requirements and deconvolution associated with directly measuring steep thermal gradients.

Proper extinguishment and thermal isolation are key factors in developing a calorimetric technique. The first series of experiments conducted in this effort involved employing depressurization to extinguish combustion. When this technique proved untenable, a second series of experiments based on burning samples down to a noncombustible base material was investigated. The reader who is only interested in an experimental technique of greater fidelity than microthermocouples will not find it in this report. However, the interplay between conduction and radiation is prominent in this work, and rough estimates of parameters such as burn rate, surface temperature, and optical absorption can be determined from the techniques and analyses described.

2. Analysis

2.1 No Radiation, Time-Independent

Assuming constant coefficients and no source terms, the time-independent heat balance in any slice of the thermal wave associated with a steady-state burning process has the form

$$k\frac{\partial^2 T(x)}{\partial x^2} - \dot{M} c_P \frac{\partial T(x)}{\partial x} = 0, \tag{1}$$

where T is the temperature, x is the direction which the propellant regresses at a constant burning rate, k is the thermal conductivity, $\dot{M}$ is the mass regression rate, and c_P is the specific heat at constant pressure. The first term represents the rate of change in heat content in the slice due to conduction; the second term is the rate of change of heat content due to mass flow. For the condensed phase, this equation can be integrated to obtain

$$T(x) - T_o = (T_s - T_o)\exp(\frac{\dot{M} c_P}{k} x), \tag{2}$$

where T_o is the initial temperature of the propellant and T_s is the surface temperature. Assuming that this is the temperature distribution in the propellant, then the total heat per unit area in the condensed phase is given by

$$Q = \int_{-\infty}^{0} (T(x) - T_o)\rho c_p dx = (T_s - T_o)\rho c_p \int_{-\infty}^{0} \exp(\frac{\dot{M} c_P}{k} x)dx, \tag{3}$$

where ρ is the propellant density. Performing the integration and rearranging yields

$$T_S = T_O + \frac{Q\dot{M}}{\rho k}. \tag{4}$$

To recast the expression in terms of experimentally measured variables, the quantity of stored heat remaining in the quenched propellant specimen is rewritten as

$$Q = (T_F - T_O)\frac{c_P m}{A_S}, \tag{5}$$

where T_F is the final, equilibrated, adiabatic temperature of the sample, m is the mass of the unburned propellant, and A_S is the area of the propellant surface that

underwent combustion. Substituting equation 5 into equation 4 and rearranging yields

$$T_S = T_O + (T_F - T_O)\frac{c_P mr}{kA_S}. \qquad (6)$$

If the thermophysical properties and the burn rate ($\dot{M} = \rho r$) of the propellant are known, a measurement of T_F from the calorimeter and A_S from the burnt surface will provide sufficient information to calculate T_S. Equation 6 is used to extract surface temperature results from experiments in which depressurization was the method of combustion extinguishment.

2.2 No Radiation, Time-Dependent

In another set of experiments, burning the propellant sample down to a noncombustible base was the method of combustion extinguishment. In these cases, the time-dependent temperature profile for a point in the base was desired. The one-dimensional heat transfer equation with steady-state conditions, constant coefficients, and no source term (as given in equation 1) yields the temperature distribution in the base $f(x) = T_o + (T_s - T_o)\exp(\frac{\rho r c_P}{k})x$ at t = 0. Assuming that the base of length L is perfectly insulated ($\frac{\partial T}{\partial x}(0,t) = \frac{\partial T}{\partial x}(L,t) = 0$), the time evolution of the profile following extinguishment can be calculated via an analytical solution given in many differential equation texts [6]

$$T(x,t) = A_O + \sum_{n=1}^{\infty} A_n \cos\frac{n\pi x}{L}\exp(\frac{-n^2\pi^2 k}{c_P\rho})t, \qquad (7)$$

where $A_O = \frac{1}{L}\int_0^L f(x)dx$, $A_n = \frac{2}{L}\int_0^L f(x)\cos\frac{n\pi x}{L}dx$, and $n = 1,2,...$

2.3 Radiation, Time-Dependent

During the course of experimental work, it was soon apparent that radiation was contributing to the measured temperature profiles. Thus, a radiative source term was added, viz.

$$k\frac{\partial^2 T}{\partial x^2} - \dot{M} c_P \frac{\partial T}{\partial x} = -\dot{Q}_R\, \alpha \exp(\alpha x), \qquad (8)$$

where an optical absorption coefficient α (cm^{-1}) has been introduced and $\dot{Q}_R$ is a radiant heat flux. This heat source term is exponentially attenuated as a function of x. The solution for equation 8 is of the same form as equation 2, but is now the sum of two exponentials. It is written as

$$T(x) - T_o = (T_s - T_o - \frac{\dot{Q}_R}{\rho c_p (r - \alpha D)}) \exp(\frac{rx}{D}) + \frac{\dot{Q}_R}{\rho c_p (r - \alpha D)} \exp(\alpha x), \quad (9)$$

where $D = \frac{k}{\rho c_p}$ is the diffusivity of the propellant. Equation 9 is still of the form $f(x)$, and may thus be used in equation 7 to obtain temperature histories for the case where there is a radiant heat source. This was facilitated by employing equation 7 as a governing equation in a multivariate least squares fitting routine to determine parameter values that yield the "best fit" to experimental data. For the particular case at hand, the fit is to the temperature at one position (the bottom center of an inert PEEK base) as a function of time. At flame extinguishment, the radiant heat source is switched off. This time can be obtained from the video record, and it manifests itself as a knee in the temperature-time history. Measured values are available for most of the parameters in equation 9, and are given later in Table 1. The condition, $r = \alpha D$ did not arise in this study with r being always greater than αD. However, as shown in Appendix A, even with $r = \alpha D$, there is a real, positive contribution from radiation. The radiative and conductive contributions (equation 9) that give rise to the increase in PEEK base temperature are also plotted as a function of distance in Appendix A.

There are several difficulties in quantifying the radiation flux, and approximations are made. First, the radiation flux and optical absorption coefficient can be wavelength dependent, but this functional dependence will not be considered here. Probably of more significance is the position or positions of the radiant heat source. There are several forms for the flame structure of solid propellants. At the lowest pressures that a propellant can burn, it may do so without establishing a visible flame. As the pressure is increased, a visible flame appears at a distance from the propellant surface. As the pressure increases more, the visible flame approaches the combusting propellant surface. Different propellants have different rates at which they approach the combusting surface as a function of pressure, as well as different final flame temperatures. These radiation flux phenomena are approximated here by a surface-positioned radiant heat source attenuated according to Beer's Law. Two adjustable parameters are employed to fit the data—the radiation flux, $\dot{Q}_R$, and an optical absorption coefficient, α. From equation 9, increasing values of the burn rate (r) cause the first term on the right to decrease exponentially (x is negative). Since r and $\dot{Q}_R$ increase with pressure, this technique will be in trouble with increasing pressure, unless the radiation contribution can be well approximated.

3. Experimental

3.1 Combustion Extinguishment by Depressurization

An existing apparatus, the mobile combustion diagnostic fixture (MCDF) [7], was used to conduct propellant surface temperature experiments where combustion was extinguished by depressurization. A sketch of the pertinent details of MCDF is shown in Figure 1. The small chamber volume is 100 cc, and the large chamber is 35,000 cc. The small chamber contains the cylindrical propellant sample, which is held in place by nylon screws. The sample is ignited when electric current is applied to a wire slightly buried at the top center of the sample. A temperature history is recorded by an Omega-manufactured, 0.075-mm wire Chromel-Alumel thermocouple. The thermocouple is placed at the bottom center of the propellant sample and a thin (~ 1 mm) propellant disk is solvent-welded to the bottom of the propellant sample to shield it from the influence of circulating gases.

A description of the experiment is given by relating the sequence of events necessary to perform an experimental run. A burst disk (for construction details, see [7]) is installed between the small and large chambers. The propellant sample is also installed and electrically connected to the ignition power supply and thermocouple readout. The large chamber is evacuated with a mechanical roughing pump and then valved off. Just prior to the igniting propellant, the small chamber is prepressurized to a value > 0.3 MPa. This pressurization insures reliable ignition and provides a baseline pressure so that the additional pressure provided by the propellant combustion gases will break the burst disk prior to completely consuming the propellant sample. The prepressurization line is valved off, and the ignition circuit is activated. Energizing the ignition circuit provides a trigger input for the dual time base Nicolet digital oscilloscope. The scope records the pressure history from a Kistler gauge and a temperature history from the thermocouple.

A typical pressure history is shown in Figure 2. Here, the small chamber was prepressurized to 0.3 MPa, and propellant combustion increases the pressure to about 2.8 MPa, at which time the burst disk functions. The gases in the small chamber rapidly vent into the large chamber. The final system pressure is close to vacuum conditions, a factor of two pressure drop occurs in a time frame of less than 0.4 ms (the time between data points is 0.2 ms). This depressurization extinguishes combustion, and the thermocouple provides a measure of the heat content of the remaining propellant sample. A representative example will be discussed in Section 4. To obtain the necessary parameters to solve equation 6 for the surface temperature, the extinguished propellant sample is weighed, and

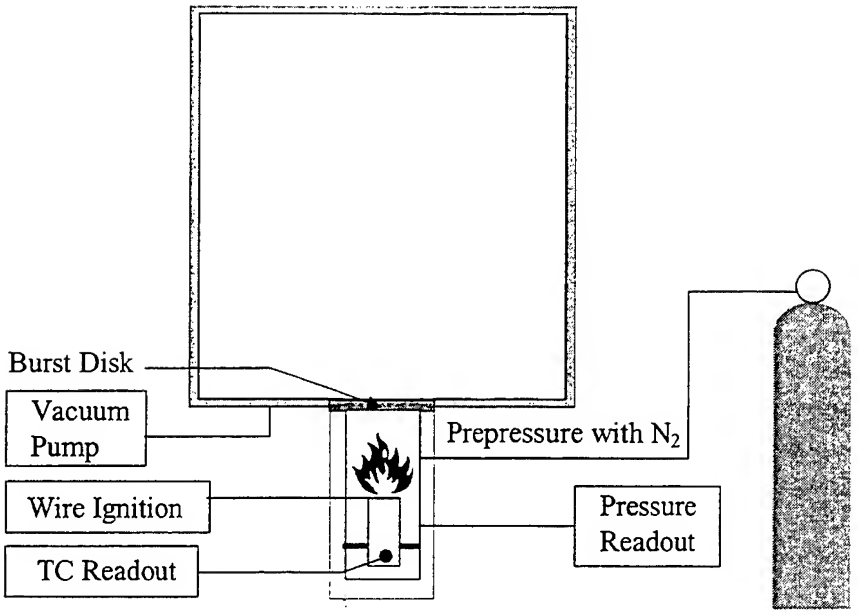

Figure 1. Sketch of the mobile combustion diagnostic facility (MCDF) apparatus configured for propellant surface temperature measurements after extinguishment by depressurization.

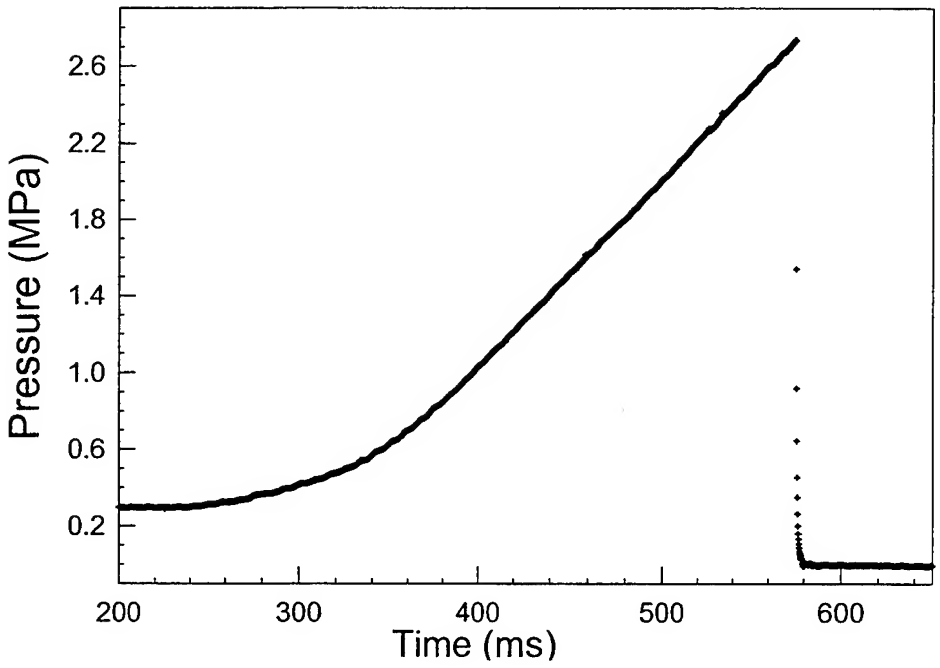

Figure 2. Typical pressure history of the MCDF experiment recorded with a Kistler gauge.

the surface area that has undergone combustion is measured. These values, together with the propellant burn rate (at the burst pressure value), specific heat, thermophysical properties, ambient temperature, and T_F (assumed to be the maximum temperature obtained from thermocouple history) were employed in equation 6 to determine the propellant surface temperature.

3.2 Combustion Extinguishment by Inert Base

The other set of experiments to measure propellant surface temperature were performed in a windowed strand burner. Briefly, this strand burner has four opposed windows through which combusting propellant samples can be illuminated, and the dynamic burning process is recorded with a video camera. The apparatus was originally developed to obtain propellant burn rate as a function of pressure for pressures up to 10 MPa. A simple sketch of the major functions of the apparatus is shown in Figure 3(a). A new feature of this experiment is the thermocouple added to record the temperature history of the inert base. Details of the first propellant sample and inert base configuration employed in the experiment are given in Figure 3(b). The inert base is made from PolyEtherEtherKetone (PEEK). This material was chosen for its ability to continuously withstand temperatures of 250 °C (and higher temperatures for a short time) and for its thermophysical properties similar to those of the solid propellants under study. Optical properties of this material are described in Appendix B. The base is a disk with the same diameter as that of the propellant sample (0.635 cm) and a nominal thickness of 0.3 cm. A 75-μ wire Chromel-Alumel thermocouple is glued to the center of the base's bottom face, and the propellant sample is solvent-welded to the top face with acetone. Times on the order of 48 hr were given for the acetone to diffuse and evaporate away before an experimental run.

The PEEK base is mounted on a Delrin stand in a way that minimizes thermal conduction. The top of the Delrin stand was machined such that three equally-spaced edge points would make contact. The bottom of the PEEK disk was edge glued to these Delrin contact points. A series of experiments were run with this configuration, but after looking at the data in detail, the effects of radiation and possibly convection were noticeable. A configuration directed at minimizing these unwanted contributions was employed. In this configuration, Figure 3(c), the Delrin stand was modified. No longer were the three points used to support the PEEK base. Instead, the top of the Delrin solid cylinder was drilled out so that a thin lip of about 0.025 cm remained, and the PEEK base was edge glued to this Delrin lip. This seal eliminated radiative contributions by reflection and convection currents around the thermocouple region. The thermocouple lead wires were covered with insulation tubing and routed down the inside of the Delrin stand. Just prior to the bottom, the leads exited a small hole that was subsequently sealed with glue. The propellant sample was hot-wire ignited by impressing a small Chromel wire into the center of its upper surface.

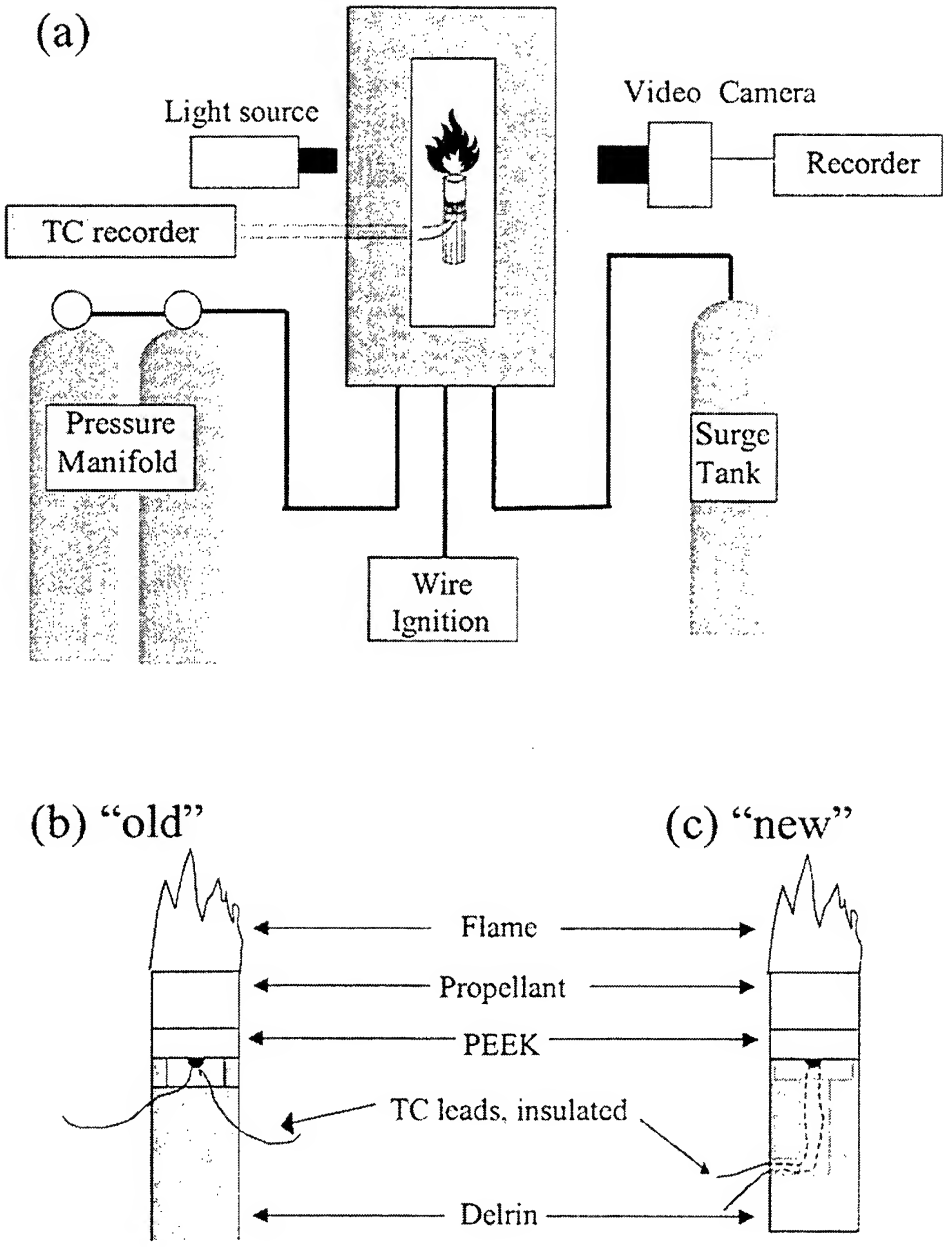

Figure 3. (a) Sketch of windowed strand burner apparatus configured for propellant surface temperature measurements after extinguishment by an inert base, (b) diagram of the propellant sample, PEEK base and delrin stand, and (c) diagram of improved base arrangement.

The sequence of events occurring in an experimental run with this apparatus is as follows. A prepared propellant sample is placed in the windowed chamber and electrically connected to the ignition power supply and thermocouple recording circuitry. Next, the chamber is closed and pressurized with nitrogen. The video camera is placed in the recording mode, and the Nicolet digital scope employed for recording the thermocouple output is triggered. Several seconds after triggering the scope, the ignition wire current supply is turned on. Combustion commences, and the regression of the combusting surface is recorded by video. The temperature history of the PEEK base is also recorded. Video records give burn rate, and the thermocouple histories provide data for heat content determinations.

4. Results

4.1 Surface Temperature From the Extinguishment by Depressurization Technique

To minimize the number of nonproductive runs when using the depressurization technique, proper initial conditions are necessary. Maximum pressure is controlled to within about ±10% by a burst disk. This pressure is provided by two sources—prepressurization with nitrogen gas and pressurization from the combustion gas. Establishing of a planar propellant burn is desired before burst disk functioning, but the disk should function prior to the thermal combustion wave reaching the embedded thermocouple. By knowing the free volume of the small chamber and propellant ingredient information, the maximum pressure can be calculated for a given mass of propellant using the NASA-Lewis code. This thermochemical equilibrium calculation [8] assumes adiabatic conditions, a poor assumption for this experiment where the combustion gas pressurization is relatively slow. In fact, for the experimental geometry and initial conditions used, the maximum pressure is about a factor of two lower than that predicted by the code. Nonetheless, the code provides a useful estimate of maximum pressure for choosing the amount of energetic material. Once a proper mass of propellant is selected, care must be taken in properly positioning and mounting the propellant sample because robust gas flow occurs after the disk bursts. Thus, designs that have minimum gas volume behind the propellant sample are necessary. Also, mounts must be made with low thermal conductivity materials, and mounting contact with the sample must be minimal to prevent substantial heat loss. On several occasions, with 0.5-in diameter propellant samples, the gas exit flow was sufficient to launch the sample from the mount, stopping only when the thermocouple leads became taut.

Representative temperature histories for experiments with XM39 and JA2 propellant samples are shown in Figure 4. For XM39, the burst disk functioned 8 s after the ignition current was applied. The maximum pressure reached was 2.4 MPa, and the temperature of the sample increased from 296.6 to 300.3 K. For JA2, the burst disk functioned 2 s after the ignition current was applied. The maximum pressure reached was 2.6 MPa, and the sample temperature increased from 296.7 to 299.3 K. Postmortem analyses of the samples determined remaining mass and combustion surface area. These values, together with thermophysical property parameters given in Table 1, are sufficient to calculate propellant surface temperatures from equation 6. Propellant surface temperature values obtained via this experiment are plotted as a function of the propellant mass regression rate in Figures 5 and 6.

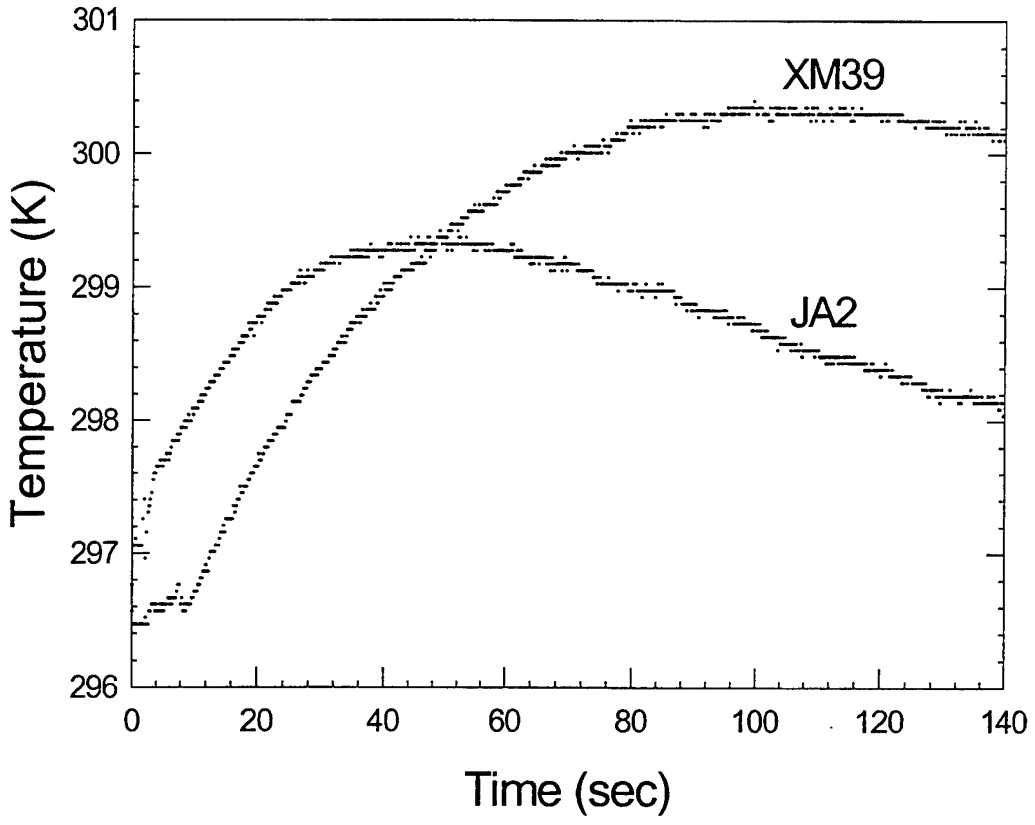

Figure 4. Temperature histories of XM39 and JA2 after extinguishment by depressurization.

Table 1. Physical properties of studied propellants and the inert base.

Parameter	Magnitude JA2[a]	XM39[b]	PEEK	Units	Reference
Length (l)	–	–	0.3	cm	
Thermal conductivity (k)	0.000694	0.000587	0.00060	cal/cm-s-K	[9, 10]
Specific heat (c_P)	0.321	0 .269	0.38	c/g-K	[9, 10]
Density (ρ)	1.57	1.64	1.286[c]	g/cm^3	[10–12]
Thermal diffusivity (D)	0.00138	0.00133	0.00123	cm^2/s	$k/c_p\rho$
Pressure (P)	–	–	–	MPa	
Burn rate (r)	$0.274P^{.83}$	$0 .05P^{.98}$	–	cm/s	[13, 14]

[a] Ingredients for JA2 are 58.2% nitrocellulose (13.04% N), 25.2% diethyleneglycoldinitrate, 15.8% nitroglycerin, and 0.05% AKARDIT II.

[b] XM39 ingredients in weight percent are 76% RDX, 12% cellulose acetate butyrate, 7.6% acetyl triethyl citrate, 4% nitrocellulose (12.6% N) and 0.4% ethyl Centralite.

[c] Measurement of weight and volume of PEEK sample.

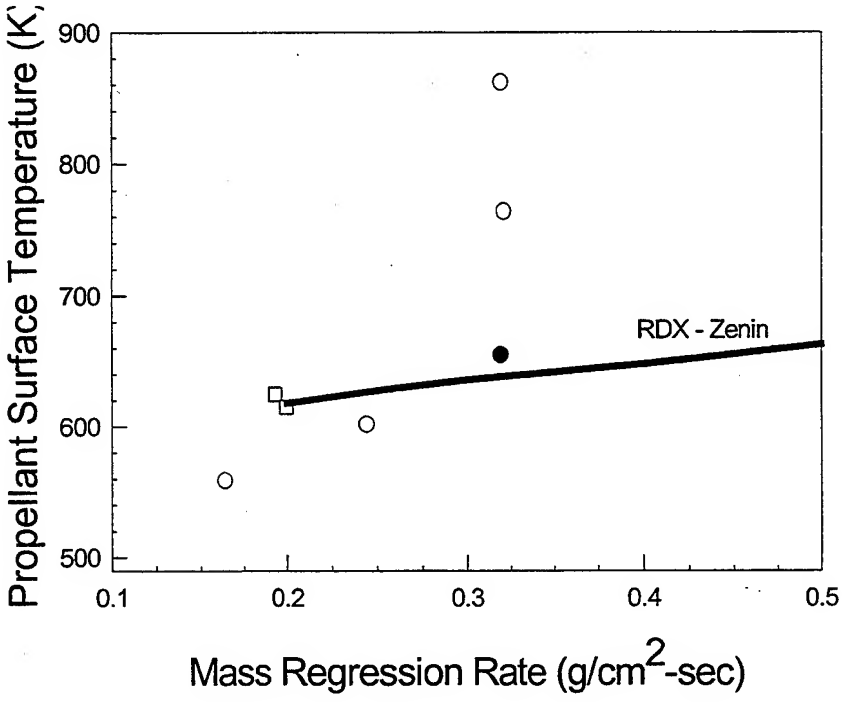

Figure 5. Propellant surface temperatures for XM39 as a function of mass regression rate. The open squares are results from depressurization extinguishment. The open circles are results from inert base extinguishment. The black circle is inert extinguishment with the improved base. For reference, the solid line represents the surface temperature for pure RDX reported by Zenin [1].

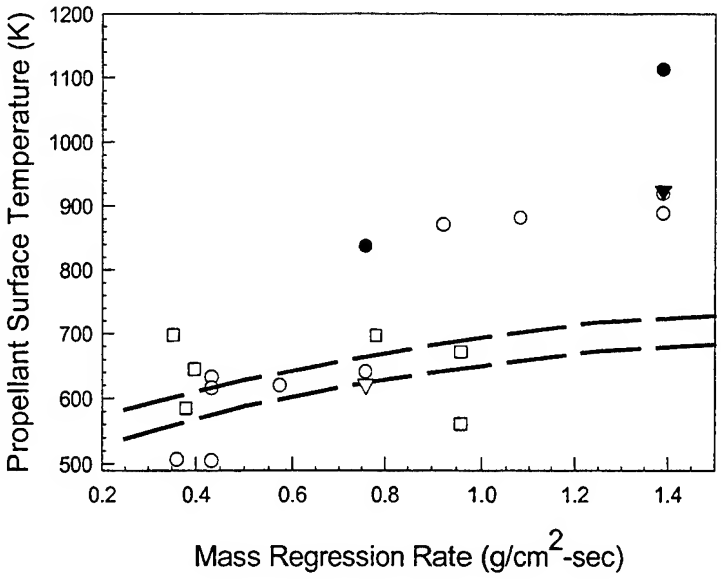

Figure 6. Propellant surface temperatures for JA2 as a function of mass regression rate. The open squares, open circles, and black circles have the same meaning as in Figure 5. The black triangle represents results with the improved base and Al foil barrier. The open triangle represents results with a JA2 base and a Mylar barrier. Upper and lower limits for double-base propellant surface temperatures reported by Zenin [1] are represented by dashed lines.

In all depressurization cases, the propellant surface was not planar at burn extinguishment. In the best cases, a hemispherical combustion surface was established. Thus, significant uncertainties in the surface area were present for many of the experimental runs. Another concern in reducing the data was the dynamics of depressurization. While depressurization was fast, whether it was fast enough that the influence on combustion kinetics was minimal prior to extinguishment is unknown. For these reasons, as well as the frequent occurrence of nonproductive runs, combustion extinguishment by burning into an inert base was pursued.

4.2 Surface Temperature From the Extinguishment by Inert Base Technique

The idea of combustion extinguishment by burning into an inert base had been thought about at the beginning of this work; however, it was assumed that heat transfer to the base via the pressurizing and combustion gases would be a large influence that could not be well quantified. Early results with the MCDF experiment demonstrated that heat loss from a propellant sample as a function of chamber pressure was not as large as assumed. With this knowledge, and the advantage of being able to simultaneously measure the burn rate with this technique, a series of inert base extinguishment experiments were conducted.

Two temperature histories of the PEEK base observed in experiments where JA2 was burned at 1 MPa and 2 MPa are shown in Figure 7. Arrows marking temperature breaks in the 2 MPa data are also included in this figure. The temperature break at 9 s marks the ignition (flame establishment) of the propellant sample, and the temperature break at about 13 s marks flame extinguishment at the inert base. What was not expected was the temperature rise in the inert base before flame extinguishment. Nonetheless, the data shows that the thermocouple temperature starts to increase as soon as the propellant flame is established and "hesitates" at flame extinguishment. Moreover, identical effects are also seen for the 1 MPa case at about 10 and 17 s, but the breaks are not as pronounced.

These observations are consistent with radiation, providing nonnegligible heating to the inert base and thermocouple. A further demonstration of this type of heating is shown in Figure 8, which is obtained from an experiment with XM39 burned at 2 MPa. Again, the thermocouple temperature starts to increase at around 9 s (flame establishment) and takes off at 29 s. Here it is not obvious where flame extinguishment takes place, but it is slightly earlier than 29 s. A closer comparison of the 2 MPa results shown in Figures 7 and 8 reveals that the early temperature rise is faster for JA2. This is because the JA2 flame is hotter and therefore brighter. For the 2 MPa case, the calculated adiabatic flame temperature for JA2 is 2800 K, whereas for XM39 it is 2355 K [8]. Another observation, consistent with radiative heating, is that when the length of the propellant sample is divided by the amount of time taken for the early temperature rise, a burn rate consistent with the video record rate is obtained. Realizing that radiation could be a substantial fraction of the total heat input into the PEEK base, it became clear that its contribution had to be included.

The simplest way to account for a radiative contribution is to use the flame extinguishment temperature value for T_o. This is a lower limit since the thermocouple indicates temperatures at the bottom of the PEEK base (see the radiation contribution plot in Appendix A). In an attempt to obtain a better account of the radiative contribution, a source term was included in the one-dimensional heat conduction equation, allowing a time-dependent solution for the temperature at any centerline depth in the PEEK base to be obtained. A multivariate least squares fitting program is used to find the best set of solution parameters for equation 7, including the propellant surface temperature.

The remainder of the temperature history data will also include a fit to the data with a reported best value for surface temperature. Initially, three experiments were conducted with JA2 at 1 MPa pressure (mass regression rate of .43 g/cm^2-s). These data are shown as open circles on Figure 6, and the parameters obtained for all fits are given in Table 2. Only the optical absorption coefficient and density were actually measured for the in-house, hot-pressed PEEK base

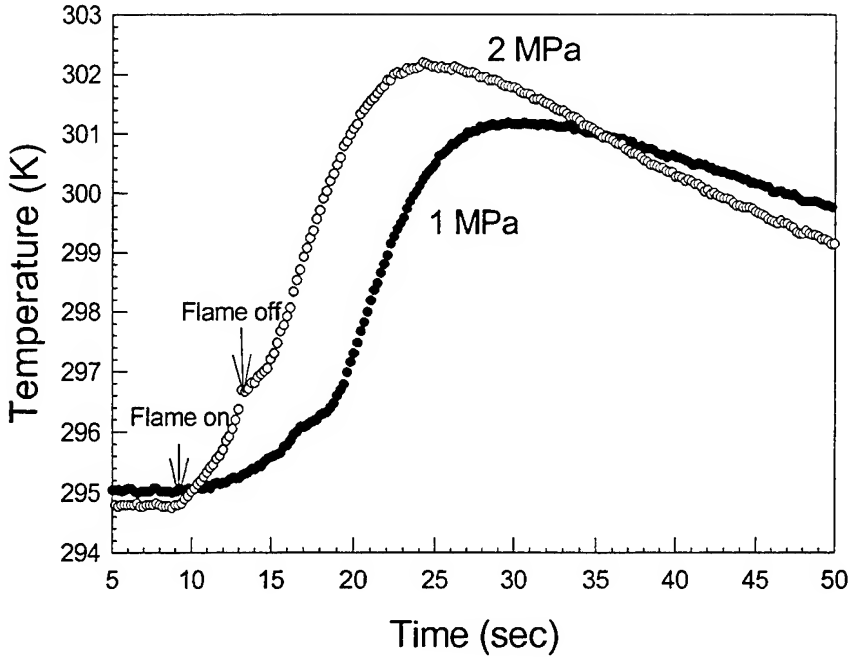

Figure 7. Temperature histories of the PEEK base (old) for JA2 burning in environments of 1 and 2 MPa nitrogen.

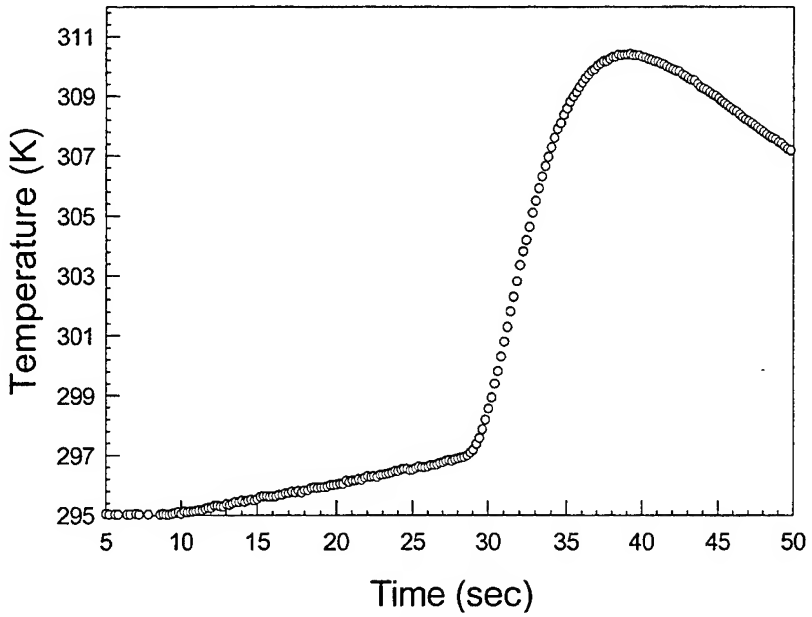

Figure 8. Temperature history of the PEEK base (old) for XM39 burning in 2 MPa nitrogen.

Table 2. Best fits for surface temperature and optical absorption coefficients for XM39 and JA2.

Prop.	Pressure (MPa)	Mass Regr. rate (g/cm^2-s)	Rad. Flux ($Cal./cm^2$-s)	Optical Abs. Coef. (cm^{-1})	Base	Surface Temp. (K)
XM39	2	0.10	0.15	0.7	old	559
"	3	0.15	0.18	1.0	old	602
"	4	0.20	0.23	1.0	old	765
"	4	0.20	0.28	1.7	old	862
"	4	0.20	0.24	0.6	new	656
JA2	0.8	0.36	0.13	1.5	old	507
"	1	0.43	0.19	0.6	old	633
"	1	0.43	0.20	1.0	old	616
"	1	0.43	0.24	1.0	old	505
"	1.4	0.57	0.31	3.0	old	620
"	2	0.76	0.70	1.3	old	641
"	2	0.76	0.30	2.6	new	837
"	2.5	0.92	0.94	1.4	old	871
"	3	1.08	0.94	1.8	old	882
"	4	1.39	0.89	1.3	old	920
"	4	1.39	0.76	1.3	old	889
"	4	1.39	0.39	1.3	new	1112
"	4	1.39	0.27	2.2	new, Al foil	924
"	4	1.39	0.32	3.4	new, aged	1683
"	2	0.76	0.62	3.2	JA2, Mylar foil	621

used; the other two parameters used to calculate the diffusivity, c_p and k, are nominal literature values. Initially, the diffusivity value of 0.00123 cm^2/s was used for PEEK, but this led to very poor fits to the data. By allowing the diffusivity to vary, a value of 0.00206 cm^2/s was obtained as a best overall fit to the data and thus was used for obtaining the values given in Table 2. Data from Figure 7, JA2 at 2 MPa, are repeated on Figure 9, and the fit to the data is shown as a solid line. Here, and in all other fits, the time history over which the data is fit has been shortened to minimize temperature-gradient-driven heat loss effects.

The parameters can be adjusted so that equation 7 represents the data well, including reproducing the observed knee at flame extinguishment. Moreover, there is a significant temperature rise prior to extinguishment at the inert base. Since this temperature rise begins with flame establishment, it is apparent that radiation is affecting the thermocouple, possibly directly impinging on the thermocouple via multiple reflections.

To minimize this effect, modifications to the inert base and thermocouple wire routing were made, and these modifications are described in the experimental section. Data taken before the modification of the base are referred to as "old" and data taken after base modification are termed "new" in Table 2. Figure 10 represents the temperature history of JA2, again at 2 MPa nitrogen pressure, obtained using the new base configuration. Here, the temperature rise before flame extinguishment is about a factor of three less than that depicted in Figure 9. Hence, radiation shielding is definitely improved. On the other hand, a best fit for surface temperature is 837 K, about 200° higher than the value found using the old base configuration. This value is much higher than literature values [1] for the surface temperature of this class of propellants.

A variety of experiments were conducted at 4 MPa, two experiments using the old base configuration and three experiments with the new base configuration. Flame extinguishment is represented by a more pronounced knee at 4 MPa, and in Figure 11 it looks more like a cusp. The best fit to surface temperature results in a very high value, 1,112 K. In an attempt to explore the radiative contribution, a 25.4 μ thick piece of aluminum foil was placed between the PEEK base and the JA2 propellant sample. The temperature history for this configuration is shown in Figure 12. The radiation component was reduced by about a factor of two, and the cusp was removed. A best fit for surface temperature is about 200 K less, but still higher than literature values. It is conjectured that in-depth absorption leads to propellant heating, which is being conducted through the Al foil barrier.

As discussed earlier, XM39 has a lower flame temperature than JA2, and the radiation contributions are expected to be less. This supposition is supported by the temperature histories shown on Figures 13–15. Figure 13 represents a temperature history for burning at 2 MPa, where the best fit for surface temperature is 559 K. Figures 15 and 16 show temperature histories for burning

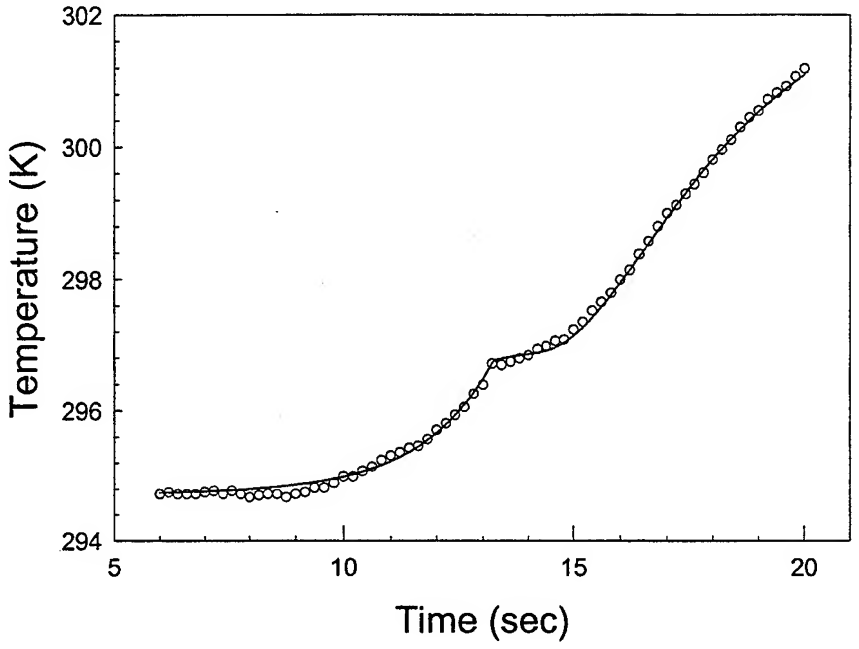

Figure 9. Temperature history data and fit for JA2 at 2 MPa.; old base configuration.

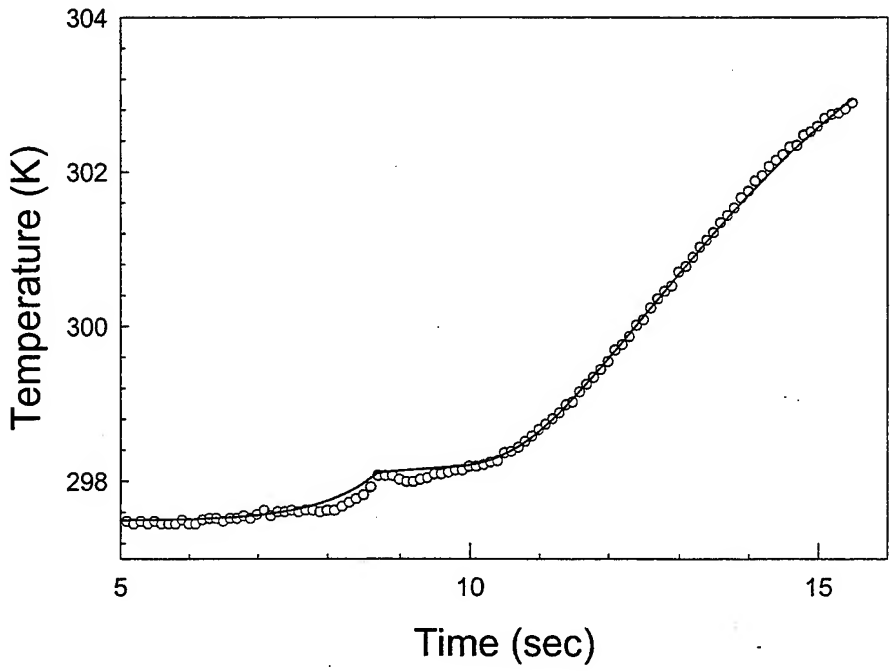

Figure 10. Temperature history data and fit for JA2 at 2 MPa; new base configuration.

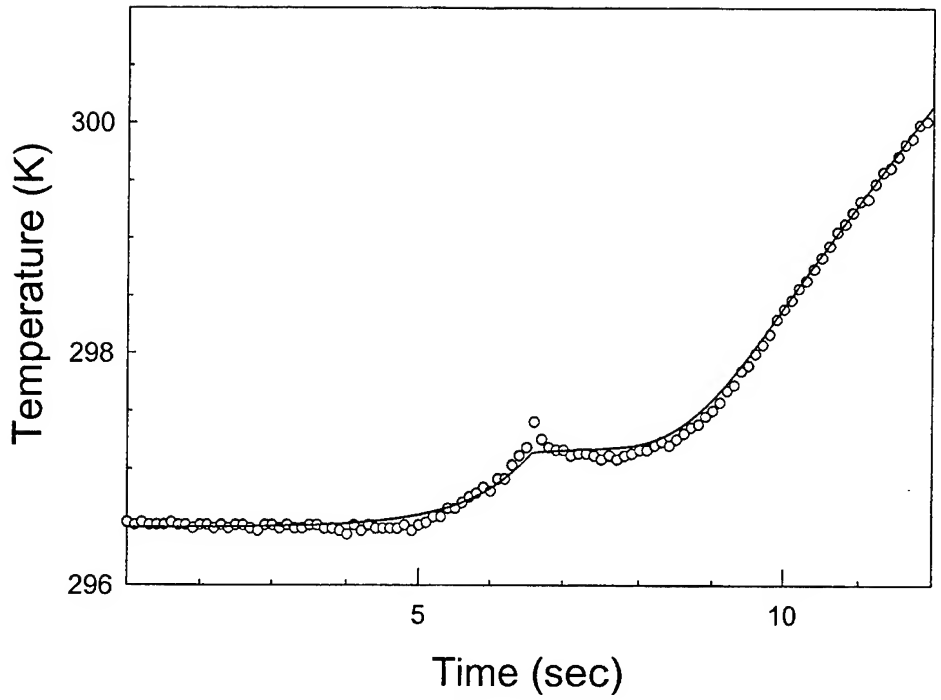

Figure 11. Temperature history data and fit for JA2 at 4 MPa; new base configuration.

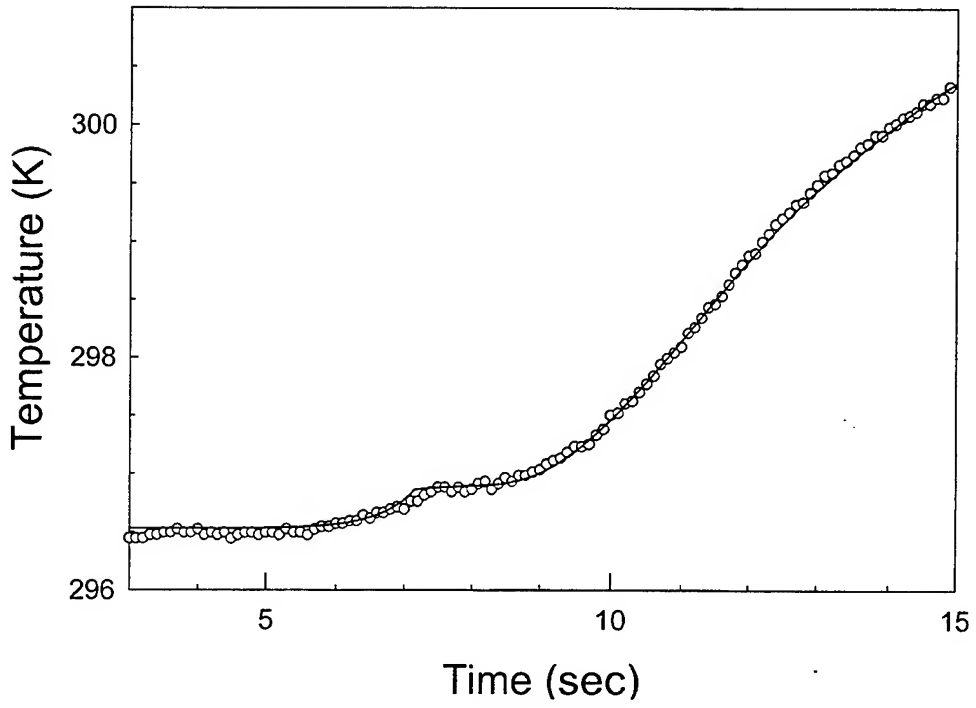

Figure 12. Temperature history data and fit for JA2 at 4 MPa; new base configuration with aluminum foil separation.

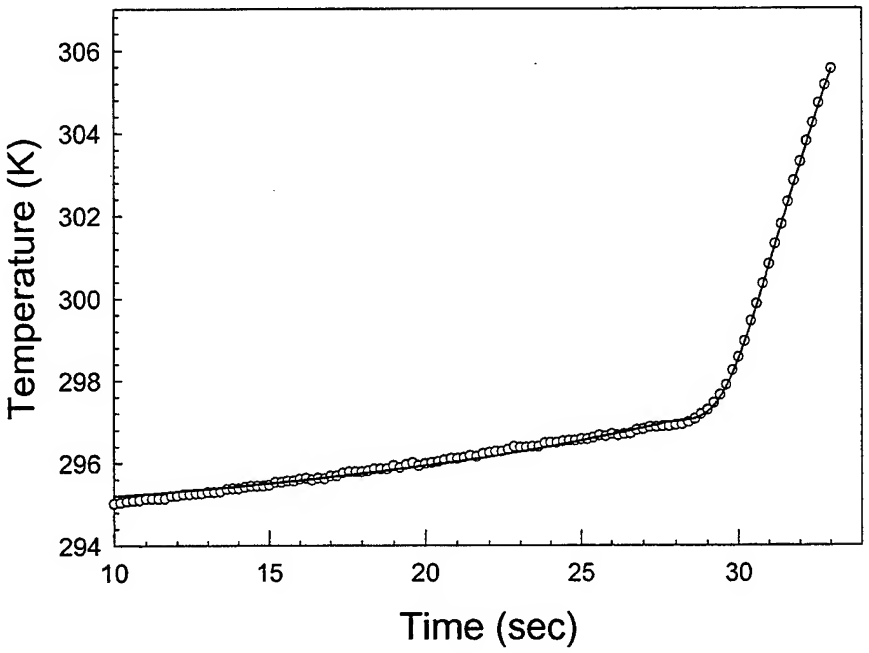

Figure 13. Temperature history data and fit for XM39 at 2 MPa; old base configuration.

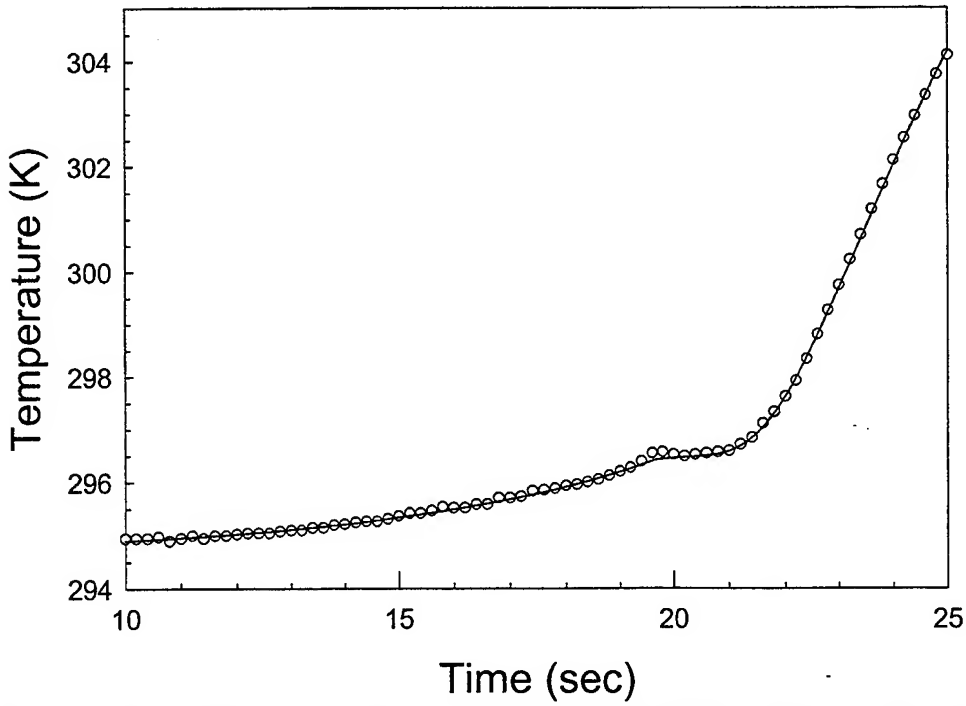

Figure 14. Temperature history data and fit for XM39 at 4 MPa; old base configuration.

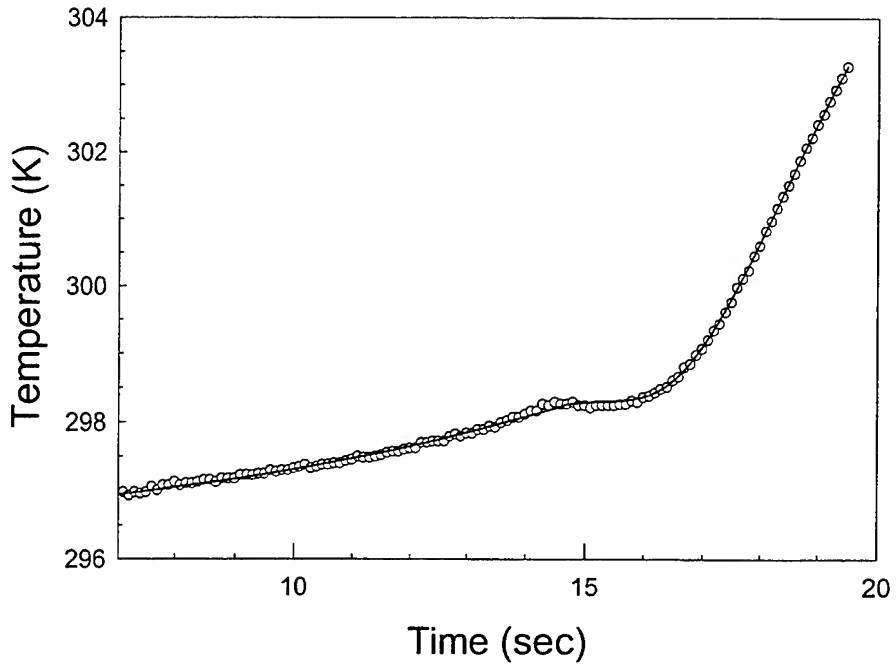

Figure 15. Temperature history data and fit for XM39 at 4 MPa; new base configuration.

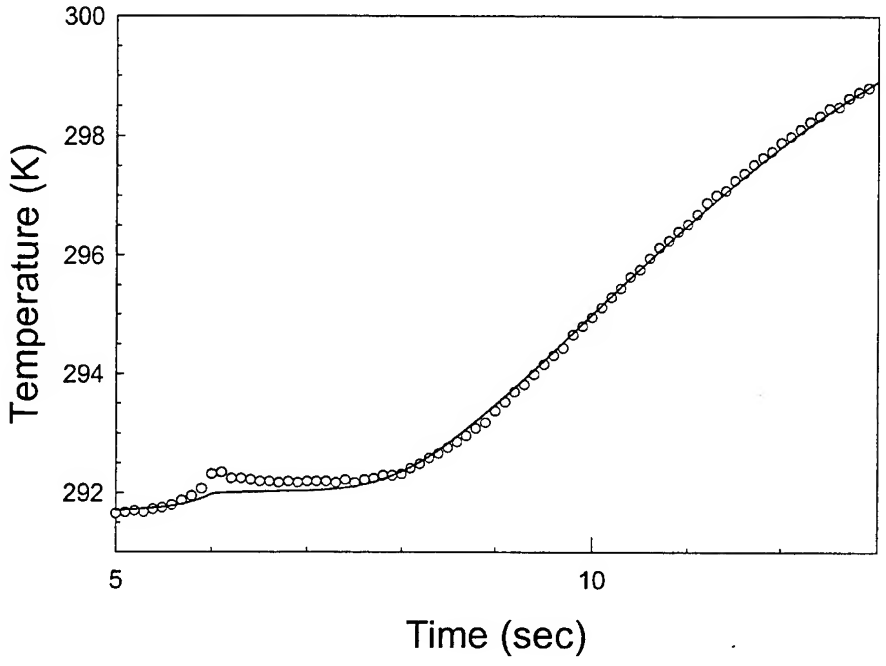

Figure 16. Temperature history data and fit for JA2 at 4 MPa; new base configuration, aged condition.

at 4 MPa, where old and new base configurations were used, respectively. The temperature histories up until flame extinguishment were almost identical in both cases, but the surface temperature determined from the new base configuration is about 100 K lower. The surface temperature with the new base is consistent with literature values for similar propellants. The implication of these results will be discussed in the next section.

A potential problem with the sample PEEK interface was uncovered by accident. Several JA2 propellant samples were not run until several months after they were prepared. A temperature history for one of these runs is displayed in Figure 16. A best fit for surface temperature results in the extraordinarily high value of 1,684 K. Furthermore, examining the top surface of the PEEK inert base showed a definite discoloration and a slight charring not seen previously. This burning presumably arises from propellant diffusion into the PEEK.

5. Discussion

Examining Figures 5 and 6, where the present results are compared to literature values of Zenin [1], reveals significant scatter and deviation. The depressurization method, abandoned for a presumably better inert base extinguishment method, displays better agreement with literature values. The scatter is distributed, more or less, uniformly about the limit lines (Figure 6). On the other hand, data obtained by inert base extinguishment, in addition to having scatter, gives larger T_S values for mass regression rates above about 0.7 g/cm^2-s. Part of the scatter can be due to a change in the base geometry. But for both cases, large T_S values were determined at the higher mass regression rates, where the radiation source is closer to the surface of the propellant.

Perhaps more problematic is that the propellants and PEEK have different optical absorption. Efforts were made to select an inert material with thermophysical properties similar to the propellants under study. This was done so that the conduction-driven thermal profile would be unperturbed, but differences in optical properties were initially considered much less important. During the course of this research, the optical absorption of PEEK was briefly investigated, and the details are given in Appendix B. The optical absorption of PEEK was substantially larger than that of JA2 or XM39. Thus, radiation can be partly absorbed by the propellant, and the remainder passing through the unburned propellant is absorbed in the PEEK base. With these considerations, it is not surprising that the simple radiation source term employed is inadequate to quantitatively account for the radiation contribution as a function of mass regression rate. Moreover, as the mass regression rate increases, both the

conductive and radiation contributions decrease, leading to a smaller experimental temperature signal.

Concern about optical property differences between the propellant and the PEEK base led to another experiment where the base material was the propellant. The problem here is stopping combustion. First, a 12.7-μ disk of Mylar was used to separate the propellant cylinders, but it did not stop the combustion wave. A thicker (38-μ) disk worked, and the temperature history data and fit are shown in Figure 17. The fit to the data provided support for the model. As opposed to fitting the experiments with a PEEK base, where the thermal diffusivity value had to be set higher than its nominal value, the Table 1 value for the thermal diffusivity of JA2 was required for a proper fit. Secondly, the obtained surface temperature of 621 K agrees with literature values. The fitted value for the optical absorption coefficient is one of the largest measured values, but it is about a factor of two lower than values reported by Cohen et al. [15].

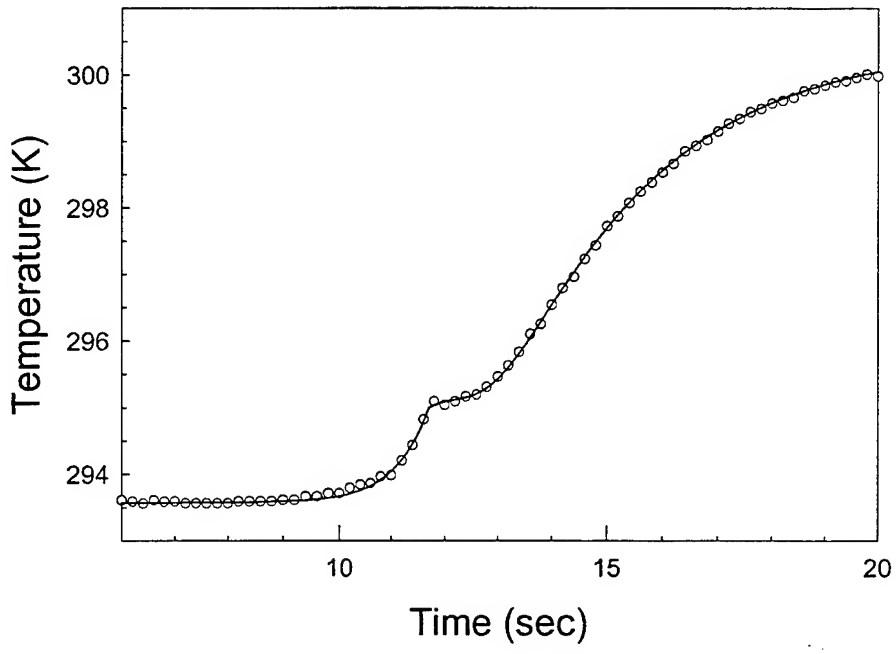

Figure 17. Temperature history data and fit for JA2 at 2 MPa.; old base configuration. In this case, the base material was JA2, and combustion was stopped by a Mylar film.

In addition to surface temperature values coming from the least squares fit of the temperature history, radiation fluxes and optical absorption coefficients are also obtained and are given in the fourth and fifth columns of Table 2. These data are somewhat scattered, but they indicate that the radiation flux is increasing with pressure, and the optical absorption coefficient of JA2 is larger than that of XM39. The larger optical absorption of JA2 is also suggested in Table B-2. In reality, the

optical absorption coefficients reported are for the combination of propellant and the PEEK base; the only exception is the experiment where JA2 was used as the base. For JA2, it also appears that the "new" base configuration has resulted in a lower radiation flux seen by the thermocouple.

Part of these results include data that can be used simply and efficiently to obtain burn rate without needing a window. An estimate of the propellant burn rate can be determined by taking the time interval from where the thermocouple temperature starts to rise until the knee in the profile, and dividing into the propellant length. For example, take the 2 MPa JA2 case shown in Figure 7. The propellant length is 2 cm, and when divided by 4.5 s, it results in a value of 0.44 cm/s. This value is close to the exponential form given in Table 1. The same result holds for the 2-cm-long XM39 sample of Figure 8.

6. Conclusions

The temperature of a propellant surface burning at atmospheric pressure can be obtained by a calorimetric technique [5]. Furthermore, the test of time has indicated that these measurements are reliable [1, 4]. Present measurements are also reliable, although somewhat scattered, near the pressure deflagration limit where the propellant burns with a wispy extended flame or no flame at all. In this region, the burn rate is low, and the heat from conduction is much larger than the radiative heat. As the pressure increases, radiative heat flux increases, and the conductive heat contribution decreases, causing the radiative component to become important. While a radiative source term has been incorporated into the heat balance, it is inadequate to handle the many variables involved with the radiative contribution, and probably necessitates matching the optical properties of the burning sample and base. Revisiting Figure 6, where the pressure variable is contained within the mass regression rate, an upper limit of about 0.7 g/cm^2-s is placed on the reliability of these techniques for obtaining the propellant surface temperature.

INTENTIONALLY LEFT BLANK.

7. References

1. Zenin, A. A. "Thermophysics of Stable Combustion Waves of Solid Propellants." *Nonsteady Burning and Combustion Stability of Solid Propellants*, edited by L. DeLuca, E. W. Price, and M. Summerfield, vol. 143, pp. 197–231, 1992.
2. Huggett, C. "Combustion of Solid Propellants." *Combustion Processes*, edited by B. Lewis, R. N. Pease, and H. S. Taylor, vol. II, pp. 514–574, 1956.
3. Kubota, N. "Combustion Mechanisms of Nitramine Composite Propellants." *The Eighteenth Symposium (Int.) on Combustion*, The Combustion Institute, pp. 187–194, 1981.
4. Klein, R., M. Mentser, G. vonElbe, and B. Lewis. "Determination of the Thermal Structure of a Combustion Wave by Fine Wire Thermocouples." *J. Phys. Chem.*, vol. 54, pp. 877–884, 1950.
5. Aristova, Z. I., and O. I. Leipunskiy. "Surface Heating of Burning Powder." *J. Phys. Chem.*, vol. 20, pp. 1391–1397, 1946.
6. Kreyszig, E. *Advanced Engineering Mathematics*, New York: John Wiley and Sons, 1962.
7. Devynck, D. "Design of a Mobile Combustion Diagnostic Fixture." BRL-MR-3412, U.S. Army Ballistic Research Laboratory, Aberdeen Proving Ground, MD, 1984.
8. Svehla, R. A., and B. J. McBride. "Fortran IV Computer Program for Calculation of Thermodynamic and Transport Properties of Complex Chemical Systems." TND-7056, National Aeronautics and Space Administration, 1973.
9. Miller, M. "Thermophysical Properties of Six Solid Gun Propellants." ARL-TR-1322, U.S. Army Research Laboratory, Aberdeen Proving Ground, MD, 1997.
10. Boedeker Plastics Incorporated. *Materials Guide*, www.boedeker.com.
11. Radford Arsenal Propellant Description Sheet. DA lot number RAD-PE-792-68, 1990.
12. Indian Head Arsenal Propellant Description Sheet. Lot number XM39-0988-100, 1990.
13. Miller, M. Updated data, 1993.

14. Teague, M. W., G. Singh, and J. A. Vanderhoff. "Spectral Studies of Solid Propellant Combustion IV: Absorption and Burn Rate Results for M43, XM39, and M10 Propellants." ARL-TR-180, U.S. Army Research Laboratory, Aberdeen Proving Ground, MD, 1993.

15. Cohen, A., J. E. Newberry, R. Kranze, K. L. McNesby, and R. A. Beyer. "Derivation of Optical Parameters From Integrating Sphere Measurements for NC Propellants." 34th JANNAF Combustion Subcommittee Joint Meeting, 27-31 October 1997.

Appendix A. Conductive and Radiative Contributions to the Thermal Combustion Wave

This appendix is provided to give the reader a feel for the implications of the model employed to reduce the experimental data and the length scales associated with typical parameters used. The main equation is equation 9 in the main body of the report, which can be rewritten as

$$T(x) - T_O = (T_S - T_O)\exp(\frac{rx}{D}) + \frac{\dot{Q}_R}{\rho c_p (r - \alpha D)}\left[\exp(\alpha x) - \exp(\frac{rx}{D})\right].$$

Applying L'Hopital's rule at $r = \alpha D$, define $f(\alpha) = \exp(\alpha x) - \exp(\frac{rx}{D})$ and

$g(\alpha) = r - \alpha D$, where $\frac{f(\alpha)}{g(\alpha)} = \frac{f'(\alpha = r/D)}{g'(\alpha = r/D)}$ in the limit of $\alpha \to r/D$.

Differentiation gives the result $\frac{x}{D}\exp(\frac{rx}{D})$, which is a real, positive contribution due to radiation.

The spatial profile of the thermal combustion wave in the PEEK base, following the burn of a JA2 sample, is plotted in Figure A-1. Both the conductive and radiative contributions are displayed. PEEK base thermophysical values (Table 1), as well as values appropriate for JA2 burning at 2 MPa (i.e., $T_s = 600$ K, $T_o = 300$ K, and $r = 0.49$ cm/s are used in equation 9 in the main body of the report. The two radiation parameters, $\dot{Q}_R$ and α, are assigned the values 0.4 cal/cm^2-s and 30 cm^{-1}, respectively. To show the radiative contribution clearly, the temperature and distance values have been truncated. At $x = 0$, the value of the temperature would be 600 K, and the thickness of the PEEK base is 0.3 cm; however, at this instant in time, the profiles do not extend that far into the base.

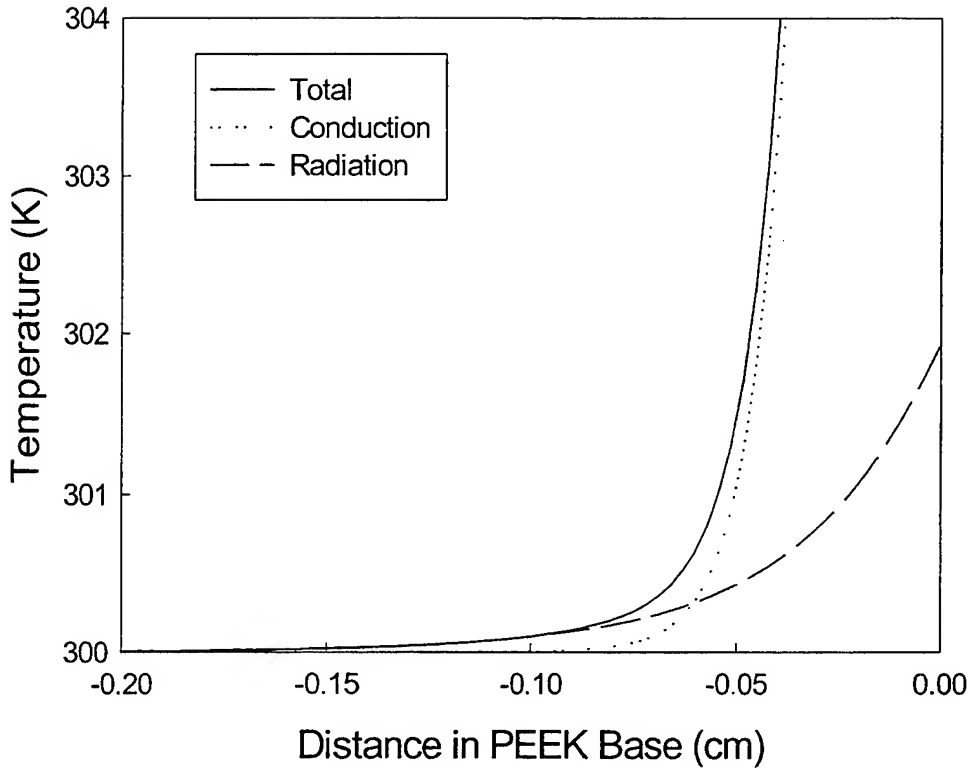

Figure A-1. Temperature vs. distance into the PEEK base for JA2 burning in an environment of 2 MPa nitrogen. Two contributions are plotted: the dashed line represents the radiative contribution, and the dotted line is the conductive contribution. The solid line is the sum of these contributions.

Appendix B. Some Properties of Unfilled PolyEtherEtherKetone

PolyEtherEtherKetone (PEEK) is a high-performance engineering thermoplastic that can be used continuously at 250 °C without permanent loss in physical properties. Some of the thermophysical properties used for calculations in the text are provided in Table 1 in the main body of the report. Values for the optical absorption coefficient for PEEK could not be found. Thus, they were measured using infrared absorption spectroscopy. A one-flux model equation of the form

$$\frac{I}{I_o} = (1 - R)\exp(-\alpha L),$$

has been used to reduce the data, where $\frac{I}{I_o}$ is the transmittance, R is the reflectivity, and α is the absorptivity. Possible scattering effects are not included in this analysis. Figure B-1 shows PEEK transmittance as a function of length (L) for three different wavelengths, and Table B-1 gives values for the reflectivity and absorptivity obtained from a regression fit to the data. These PEEK values are for bulk absorption, as they are taken in spectral regions of no apparent specific molecular absorption.

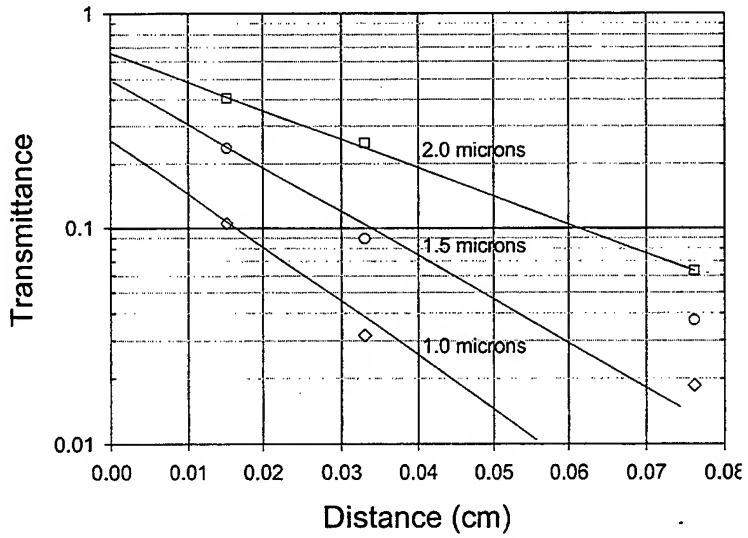

Figure B-1. A semilog plot of optical transmittance vs. PEEK material thickness for three wavelengths.

Table B-1. Optical properties of unfilled PEEK, JA2, and XM39.

Material	Wavelength (microns)	Reflectivity	Absorptivity (cm^{-1})
PEEK	1	.74	60
PEEK	1.5	.51	48
PEEK	2.0	.36	29
JA2[1]	1.06	0.04	9
JA2[1]	1.71	0.03	13
XM39[2]	0.53	0.99	8

[1] Cohen, A., J. E. Newberry, R. Kranze, K. L. McNesby, and R. A. Beyer. "Derivation of Optical Parameters From Integrating Sphere Measurements for NC Propellants." 34th JANNAF Combustion Subcommittee Joint Meeting, 27-31 October 1997.

[2] Stufflebeam, J. H. "Surface and Gas-Phase Diagnostics for Solid Propellant Combustion." U.S. Army Research Office Progress Report, Contract: DAAH04-94-C-0076, 28 November 1997. (These values are for RDX. XM39 contains 76% RDX by weight.)

NO. OF COPIES	ORGANIZATION
2	DEFENSE TECHNICAL INFORMATION CENTER DTIC DDA 8725 JOHN J KINGMAN RD STE 0944 FT BELVOIR VA 22060-6218
1	HQDA DAMO FDT 400 ARMY PENTAGON WASHINGTON DC 20310-0460
1	OSD OUSD(A&T)/ODDDR&E(R) R J TREW THE PENTAGON WASHINGTON DC 20301-7100
1	DPTY CG FOR RDA US ARMY MATERIEL CMD AMCRDA 5001 EISENHOWER AVE ALEXANDRIA VA 22333-0001
1	INST FOR ADVNCD TCHNLGY THE UNIV OF TEXAS AT AUSTIN PO BOX 202797 AUSTIN TX 78720-2797
1	DARPA B KASPAR 3701 N FAIRFAX DR ARLINGTON VA 22203-1714
1	US MILITARY ACADEMY MATH SCI CTR OF EXCELLENCE MADN MATH MAJ HUBER THAYER HALL WEST POINT NY 10996-1786

NO. OF COPIES	ORGANIZATION
1	DIRECTOR US ARMY RESEARCH LAB AMSRL D D R SMITH 2800 POWDER MILL RD ADELPHI MD 20783-1197
1	DIRECTOR US ARMY RESEARCH LAB AMSRL DD 2800 POWDER MILL RD ADELPHI MD 20783-1197
1	DIRECTOR US ARMY RESEARCH LAB AMSRL CI AI R (RECORDS MGMT) 2800 POWDER MILL RD ADELPHI MD 20783-1145
3	DIRECTOR US ARMY RESEARCH LAB AMSRL CI LL 2800 POWDER MILL RD ADELPHI MD 20783-1145
1	DIRECTOR US ARMY RESEARCH LAB AMSRL CI AP 2800 POWDER MILL RD ADELPHI MD 20783-1197
	ABERDEEN PROVING GROUND
4	DIR USARL AMSRL CI LP (BLDG 305)

NO. OF
COPIES ORGANIZATION

ABERDEEN PROVING GROUND

31 DIR USARL
AMSRL WM BD
W R ANDERSON
R A BEYER
A BIRK
A L BRANT
S W BUNTE
C F CHABALOWSKI
L M CHANG
T P COFFEE
J COLBURN
P J CONROY
R A FIFER
B E FORCH
B E HOMAN
S L HOWARD
P J KASTE
A J KOTLAR
C LEVERITT
K L MCNESBY
M MCQUAID
M S MILLER
T C MINOR
A W MIZIOLEK
J B MORRIS
J A NEWBERRY
M J NUSCA
R A PESCE-RODRIGUEZ
G P REEVES
B M RICE
R C SAUSA
J A VANDERHOFF
A W WILLIAMS

REPORT DOCUMENTATION PAGE

Form Approved
OMB No. 0704-0188

1. AGENCY USE ONLY *(Leave blank)*	2. REPORT DATE	3. REPORT TYPE AND DATES COVERED
	March 2001	Final, October 1998–October 2000

4. TITLE AND SUBTITLE
On Propellant Surface Temperatures Derived From Calorimetry

5. FUNDING NUMBERS
622618.H80

6. AUTHOR(S)
John A. Vanderhoff and Michael McQuaid

7. PERFORMING ORGANIZATION NAME(S) AND ADDRESS(ES)
U.S. Army Research Laboratory
ATTN: AMSRL-WM-BD
Aberdeen Proving Ground, MD 21005-5069

8. PERFORMING ORGANIZATION REPORT NUMBER
ARL-TR-2434

9. SPONSORING/MONITORING AGENCY NAMES(S) AND ADDRESS(ES)

10.SPONSORING/MONITORING AGENCY REPORT NUMBER

11. SUPPLEMENTARY NOTES

12a. DISTRIBUTION/AVAILABILITY STATEMENT
Approved for public release; distribution is unlimited.

12b. DISTRIBUTION CODE

13. ABSTRACT *(Maximum 200 words)*

Propellant surface temperatures for double base (JA2) and nitramine (XM39) propellant samples burning at pressures from 0.8 to 4 MPa have been measured using two different calorimetric techniques. The methods differ in the way combustion is extinguished; one involves depressurization, and the other involves burning into an inert base. For the experiments based on depressurization, a main source of uncertainty was in determining the area of the combusting surface. Moreover, this technique was prone to a large number of unproductive runs. Most of the data presented here was obtained from experiments in which combustion was extinguished by burning into a PolyEtherEtherKetone (PEEK) base. This robust material has thermophysical properties similar to the propellants studied. At higher pressures (and mass regression rates), radiative heating made nonnegligible contributions to total heat input to the inert base. Thus, a multivariate least squares model was developed to describe a time-dependent radiative and conductive heat input, and it was used to fit the experimental temperature histories. Propellant surface temperatures, radiative fluxes, and optical absorption coefficients are obtained from the fit to the data. For the regions of low mass regression rates (< 0.7 g/cm^2-s), the propellant surface temperatures were in agreement with published values. At larger mass regression rates, the propellant surface temperatures were larger than published values. This was believed to be a consequence of the way contributions from radiative heating were treated.

14. SUBJECT TERMS
propellant surface temperature, radiative heating, heat conduction, propellant burning

15. NUMBER OF PAGES
41

16. PRICE CODE

17. SECURITY CLASSIFICATION OF REPORT	18. SECURITY CLASSIFICATION OF THIS PAGE	19. SECURITY CLASSIFICATION OF ABSTRACT	20. LIMITATION OF ABSTRACT
UNCLASSIFIED	UNCLASSIFIED	UNCLASSIFIED	UL

INTENTIONALLY LEFT BLANK.

USER EVALUATION SHEET/CHANGE OF ADDRESS

This Laboratory undertakes a continuing effort to improve the quality of the reports it publishes. Your comments/answers to the items/questions below will aid us in our efforts.

1. ARL Report Number/Author ARL-TR-2434 (Vanderhoff) Date of Report March 2001

2. Date Report Received _____

3. Does this report satisfy a need? (Comment on purpose, related project, or other area of interest for which the report will be used.) _____

4. Specifically, how is the report being used? (Information source, design data, procedure, source of ideas, etc.) _____

5. Has the information in this report led to any quantitative savings as far as man-hours or dollars saved, operating costs avoided, or efficiencies achieved, etc? If so, please elaborate. _____

6. General Comments. What do you think should be changed to improve future reports? (Indicate changes to organization, technical content, format, etc.) _____

CURRENT ADDRESS

_____
Organization

_____
Name E-mail Name

_____
Street or P.O. Box No.

_____
City, State, Zip Code

7. If indicating a Change of Address or Address Correction, please provide the Current or Correct address above and the Old or Incorrect address below.

OLD ADDRESS

_____
Organization

_____
Name

_____
Street or P.O. Box No.

_____
City, State, Zip Code

(Remove this sheet, fold as indicated, tape closed, and mail.)
(DO NOT STAPLE)

DEPARTMENT OF THE ARMY

OFFICIAL BUSINESS

NO POSTAGE
NECESSARY
IF MAILED
IN THE
UNITED STATES

BUSINESS REPLY MAIL
FIRST CLASS PERMIT NO 0001,APG,MD

POSTAGE WILL BE PAID BY ADDRESSEE

DIRECTOR
US ARMY RESEARCH LABORATORY
ATTN AMSRL WM BD
ABERDEEN PROVING GROUND MD 21005-5066